Correlation between Energy, Polarizability, and Hardness Profiles in the Isomerization Reaction of HNO and ClNO

E. Sicilia and N. Russo*

Dipartimento di Chimica, Universita' della Calabria, I-87030 Arcavacata di Rende (CS), Italy

T. Mineva

Institute of Catalysis, Bulgarian Academy of Sciences, bul G. Bonchev bl.11, 1113 Sofia, Bulgaria

Received: June 30, 2000; In Final Form: October 16, 2000

The validity of the maximum hardness and minimum polarizability principles has been tested for HNO and ClNO isomerization reactions. The former can be considered as a prototype of a two-state reaction and the latter as an example of reaction involving a system with a strong ionic character. For HNO both the $^1A'$ and $^3A''$ states have been considered. The hardness values along the reaction paths have been calculated by employing several working definitions and functionals in the framework of density functional theory. The correspondence between the profiles of hardness, polarizability, and energy has been investigated as a function of the reaction coordinate or the bond angle variation. The constancy of chemical potential has also been taken into account. No obvious relation between hardness or polarizability and energy profiles and between hardness and polarizability profiles has been observed.

1. Introduction

Qualitative concepts such as electronic chemical potential (μ), molecular softness (S) and hardness (η),[1,2] widely used intuitively by the chemists to rationalize and predict various physicochemical phenomena, have found their rigorous theoretical definition within density functional theory (DFT).[1] It has been demonstrated by Parr and co-workers[3] that the chemical potential and the hardness represent the first- and the second-order derivatives, respectively, of the energy (E) with respect to the number of electrons (N) and then provide information about the response of the whole system to a change in the number of electrons at fixed external potential ($v(\mathbf{r})$). For a molecular or atomic system, these derivatives are difficult to evaluate, and therefore, to this purpose several operational definitions have been proposed. Most of these working formulas, in the framework of DFT[1,3−6] as well of Hartree−Fock[7] or semiempirical[8] techniques, are based on the finite difference approximation, in which usually a change of an integer one electron is involved. Since the exact definition of μ and η demands that the derivatives are taken for an infinitesimally small change in N, consideration of $\Delta N = \pm 1$, often leads to chemically inconsistent interpretations, even when these quantities are employed in a qualitative analysis.[9,10] Although it is possible that, within Janak's extension of DFT, a noninteger change of the electrons can be made. Using this theoretical background, computational schemes, dealing with fractional occupation numbers for hardness[12,13] and for chemical potential[13] evaluation, have been proposed and applied in the rationalization of various chemical and physical problems.[14−20] An exhaustive description of the phenomena for which the concepts of hard and soft are successfully applied can be found in the recent monograph of Pearson.[21]

The possibility to define rigorously and to assign numbers to the reactivity indicies has permitted the statement of several principles involving the reactivity indices variation during the reaction.[4,5,22,23]

As motivated by a statement of Pearson,[4,5] "It seems to be a rule of nature that molecules arrange themselves so as to be as hard as possible", the molecular hardness can be conceived as a measure of the stability of a system. As a consequence of this maximum hardness principle (MHP),[24,25] since a chemical species is most reactive at the transition state, hardness would attain a minimum there, along a reaction path. The MHP has received much recent attention, but it is still not completely understood. A formal statistical−mechanical proof that demands the constraint of constant chemical potential has been given by Parr and Chattaraj.[24] It has been further examined within the Gyftopoulos−Hatsopoulos three-level model,[26] but a lack of universal validity of an unconstrained MHP has been at the same time pointed out.[27] Furthermore, a favorable viewpoint of MHP has been obtained by Liu and Parr.[28] In the meantime, a great deal of work has been devoted to the numerical study of the MHP.[22,23,29−45] The main conclusion of these studies is that, notwithstanding, the MHP is potentially a powerful tool, and the conditions of its applicability and, then, of constructing a hardness profile similar to an energy one are not well understood.

The alternative response function to hardness corresponding to the change of energy with respect to the external potential $v(\mathbf{r})$ at fixed N represents the polarizability (α). It has been shown[46,47] that the atomic softnesses are linearly correlated with the atomic polarizabilities. Since the softness is the inverse of the hardness,[2] an inverse relationship between hardness and polarizability has been established through DFT,[48] and as a consequence of the MHP, a minimum polarizability principle (MPP) has been formulated.[22] In analogy to the MHP, since a species is most polarizable at the transition state, polarizability would attain a maximum there.

10.1021/jp002350d CCC: $20.00
Published on Web 12/15/2000

The results of the numerous studies about the MHP have pointed out that in many cases the hardness profile goes through a minimum near the transition state along the reaction coordinate and the constraint of constant μ is not a severe condition. On the other hand, on many occasions, no minimum has been found near the transition state. Less numerous are the investigations,[31,41−43,45,49] about the relationship between hardness and polarizability and the validity of the minimum polarizability principle. We would like to underline that if the hardness does not follow precisely the MHP at nonconstant chemical potential, it is highly probable that also the MPP is not obeyed. Differences in the behavior of η and α could be ascribed to the different level of numerical approximation used for their calculations, notwithstanding that finite difference formula are adopted for obtaining both the quantities. Generally, much more experience has been accumulated for the polarizability calculations,[50] which has led to refining the numerical procedures for α, while for the hardness and softness often rough approximations have been used and only in the most recent literture more sophisticated algorithms have been proposed and applied.[13−20,51] However, much more work is needed to get knowledge of how the basis set quality and the level of exchange-correlation functionals influence the reactivity index values.

Because of the aforesaid reasons and of the small number of applications to isomerization reactions occurring with mechanisms other than internal rotations, it is interesting to explore different situations such as isomerizations involving internal shifts. In this work, we have examined the variation of hardness, calculated by using different work definitions, polarizability, energy and chemical potential along the reaction path for the isomerization reactions of HNO and ClNO, with the aim to extend the previously started study[38,40] of the validity of the MHP and MPP. Following the indications coming from a previous work on HNO,[36] for this system we have considered both $^1A'$ and $^3A''$ states. Since Parr and Gazquez[52] have pointed out that hardness is at an extremum at any point where both electronic energy (E_{el}) and nuclear repulsion energy (V_{nn}) reach respective extremum values, also the behavior of these two quantities has been examined along the reaction coordinate.

2. Method

Incorporation of the concepts of hardness and softness (S) into DFT has led to the mathematical definition of η as the second derivative of the total energy with respect to the number of electrons N:[3,53]

$$\eta = \left[\frac{\partial^2 E}{\partial N^2}\right]_{v(\mathbf{r})} \tag{1}$$

or, equivalently,

$$\eta = \left[\frac{\partial \mu}{\partial N}\right]_{v(\mathbf{r})} \tag{2}$$

where the chemical potential, μ, is the first derivative of the total energy relative to the electron number. Therefore, using three-point finite difference approximation for the energy derivatives, the chemical potential and the hardness may be written as

$$\mu_{IA} = -\frac{I + A}{2} \tag{3}$$

$$\eta_{IA} = -\frac{I - A}{2} \tag{4}$$

where I is the first ionization potential and A is the electron affinity. We would like to note, that the $^1/_2$ factor in the hardness definiton is omitted in the IRHT working formula used for η calculations throughout this paper.

In the context of molecular orbital theory, by using Koopmans approximation (HL), eqs 3 and 4 can be further simplified using for I and A, the negative of the eigenvalues (ϵ) of the highest occupied (HOMO) and the lowest unoccupied (LUMO) orbitals. The use of ϵ_{HOMO} and ϵ_{LUMO} is not recommended for species with a close to zero HOMO−LUMO energy gap and when it is necessary to consider the influence of other orbitals, besides the HOMO and LUMO's. Furthermore, in the above formula the change of an integer one electron is considered and, as it was already mentioned, an inconsistent behavior of the reactivity indicies can be observed.[9,20]

Another point that needs to be considered is the fact that the Kohn−Sham (KS) orbitals are different from the canonical molecular orbitals.[1] The meaning of the KS orbitals is a subject of discussion[54−56] from the beginning of the utilization of DFT. Stowasser and Hoffmann[56] have pointed out that, although the number, symmetry, properties, and shape of KS orbitals are correct, to go beyond a qualitative interpretation it is necessary to apply a suitable scaling. This is also true for hybrid functionals. However, the working formula for the reactivity indices calculation within DFT operates mostly with the orbital energy differences, and the computations provided by Stowasser and Hoffmann[56] have demonstrated that the relative spacing of the electronic levels remains approximately constant for all the wave functions and for all the exchange-correlation functionals employed in their study.

To calculate hardness in its "natural" DF framework, a method[40] for the construction of the internally resolved hardness tensor (IRHT) in the framework of DFT formalism, yet proven successful, has been employed. Details of this method can be found in refs 23 and 37, but for easier reading, we will sketch below the main scheme of the IRHT algorithm.

The generalization of Slater's[57] transition state approach through the Janak's theorem

$$\epsilon_i = \left(\frac{\partial E}{\partial n_i}\right)_{i=1,...,N} \tag{5}$$

has introduced the possibility to extend DFT also for noninteger occupation numbers and has provided the physical and mathematical justification for expanding the energy functional in a Taylor series around the state characterized by the corresponding set of occupation numbers n^0 (n_1^0, n_2^0, ..., n_k^0) and by the corresponding KS-eigenvalues $\epsilon^0 = (\epsilon_1^0 ... \epsilon_k^0)$. In this series, the first derivatives of the energy functional with respect to the occupation numbers have the meaning of the KS-eigenvalues (see eq 5), and the second derivatives

$$\frac{\partial^2 \mathrm{E}}{\partial \mathrm{n}_i \partial \mathrm{n}_j} = \eta_{ij} \tag{6}$$

give the hardness matrix elements as defined by Liu and Parr.[58]

Having eqs 5 and 6 in mind, it is easy to express the hardness matrix elements as the derivatives of the KS-orbitals (i.e. the ijth element of the hardness matrix can be now obtained as the first derivative of ϵ_i with respect to n_j):[12,40]

$$\eta_{ij} = \frac{\partial \epsilon_i}{\partial \mathrm{n}_j} \tag{7}$$

and to approximate them numerically using the finite difference

formula:

$$\eta_{ij} = \frac{\epsilon_i(n_j - \Delta n_j) - \epsilon_i(n_j)}{\Delta n_j} \tag{8}$$

The latter expression takes into account the energy variation of the *i*th orbital due to the *j*th occupation number variation.

From the hardness matrix one can calculate the total hardness value going through the calculation of the softness matrix. It is noteworthy that the local hardness and softness are reciprocal to each other[1] and the softness matrix is the inverse of the hardness one:

$$[s_{ij}] = [\eta_{ij}]^{-1} \tag{9}$$

Since the total softness is obtained as an integral of the local softness and the total softness is an additive function of $s(r)$, S is obtained from the following approximation:

$$S = \sum_{ij} s_{ij} \tag{10}$$

Now the total hardness becomes

$$\eta = \frac{1}{S} = \frac{1}{\sum_{ij} s_{ij}} \tag{11}$$

Polarizability is calculated, according to the following equation,

$$\alpha = 1/3(\alpha_{xx} + \alpha_{yy} + \alpha_{zz}) \tag{12}$$

as the arithmetic average of the three diagonal elements of the polarizability tensor, the α_{ii} being obtained through the finite field method.[59]

3. Computational Details

The computational method used for geometry optimization and frequency calculations was density functional theory in its B3LYP[60,61] formulation in conjunction with the 6-311++G** basis set. To follow the variation of the energy, polarizability, and the other quantities of interest along the reaction coordinate, intrinsic reaction coordinate (IRC) pathways have been constructed starting from the appropriate transition state. For some selected point along the IRC, electronic properties have been computed. All these computations have been carried out using the Gaussian94[62] code.

Energy, hardness, and chemical potential profiles have been also constructed using the Perdew and Wang exchange[63] and Perdew correlation[64] functionals (PWP86) and the triple-ζ quality basis sets given by Goudbot et al.[65] as implemented in a modified version of deMon code.[66] To locate the extreme points on the potential energy hypersurface, the Broyden−Fletcher−Goldfarb−Shanno minimization algorithm[67] for the minima has been used. For the saddle points search, the Abashkin and Russo[68] algorithm has been employed. The points along the reaction paths have been obtained by fixing the appropriate geometrical parameter and optimizing all the others. To use the IRHT approach, the calculations of the hardness matrix elements and, consequently, of the absolute hardness values have been carried out by taking into account only the occupied valence orbitals and setting the variation of the occupation number Δn_j equal to 0.15. In both cases, the vertical values of *I* and *A* have been calculated by the energy difference method, where separate calculations are carried out for the neutral species and its ions.

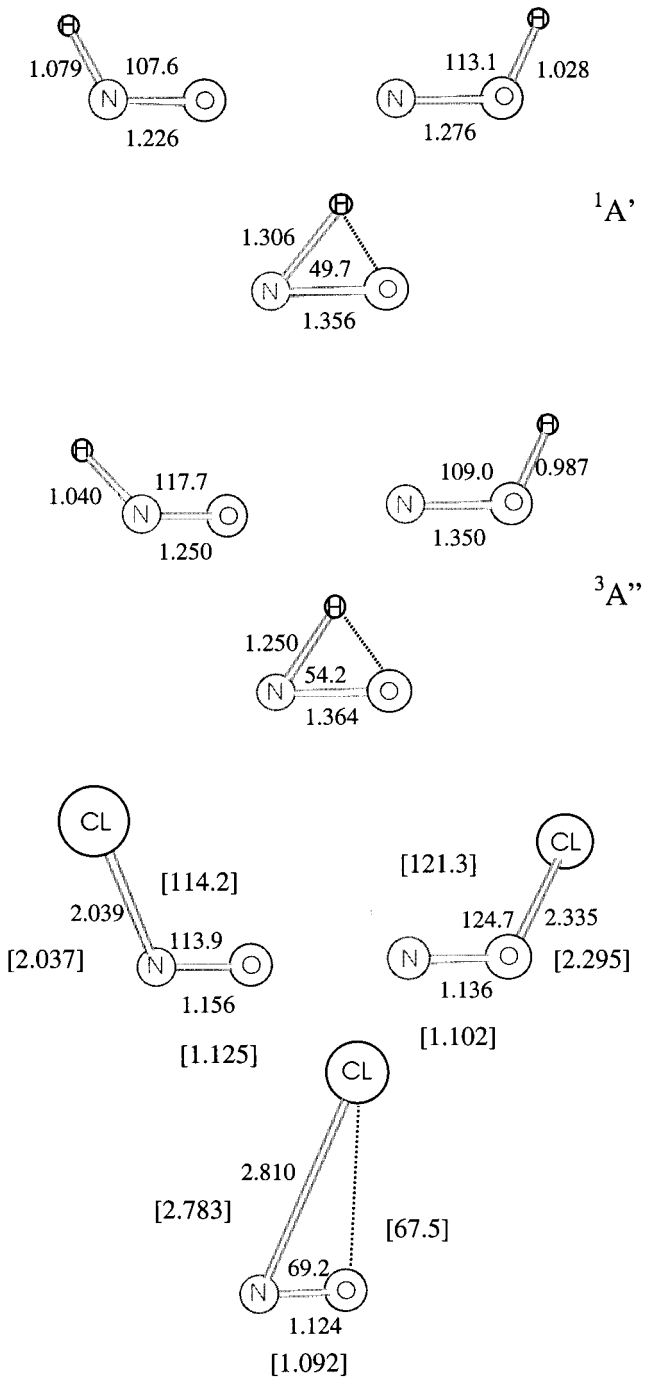

Figure 1. PWP86 geometrical parameters for HNO and HON isomers, both ^{1}A′ and ^{3}A″ states, for ClNO and ClON isomers and transition states between them. In parentheses are reported B3LYP values. Bond distances are in Å and angles in degrees.

4. Results and Discussion

The optimized PWP86 geometries of HNO and ClNO isomers and transition states for the isomerization reactions are reported in Figure 1. In the same figure are reported optimized B3LYP geometrical parameters for species involved in the ClNO isomerization reaction, while for HNO isomerization optimized geometries are summarized in ref 36. The DF structural parameters are in good agreement with available experimental data[69−71] and close to the results obtained by the post-Hartree−

TABLE 1: B3LYP Total Energy (E), Calculated Hardness from HOMO−LUMO Energy Gap (η_{HL}), IP and EA Finite Difference (η_{IA}), and Polarizability (α)[a]

system	E	η_{HL}	η_{IA}	α
HNO(^{1}A′)	−130.511 528	1.878	4.718	10.438
TS	−130.391 392	1.252	4.192	10.326
HON(^{1}A′)	−130.446 685	1.415	4.184	10.667
HNO(^{3}A″)	−130.495 923	1.477	5.209	10.336
TS	−130.423 988	2.056	5.796	10.512
HON(^{3}A″)	−130.479 451	2.252	5.852	10.074
ClNO	−590.157 027	1.994	5.383	23.678
TS	−590.103 843	0.919	3.611	29.408
ClON	−590.116 364	1.329	4.065	29.674

[a] Total energy is in au, hardness in eV, and polarizability in au.

TABLE 2: PWP86 Total Energy (E) and Calculated Hardness from Internally Resolved Hardness Tensor (η_{IRHT}), HOMO−LUMO Energy Gap (η_{HL}), and IP and EA Finite Difference (η_{IA})[a]

system	E	η_{IRHT}	η_{HL}	η_{IA}
HNO(^{1}A′)	−130.657 911	6.208	0.530	5.258
TS	−130.545 498	6.184	0.040	4.640
HON(^{1}A′)	−130.592 322	5.961	0.058	4.612
HNO(^{3}A″)	−130.641 269	5.935	0.139	4.831
TS	−130.572 145	5.527	0.620	5.338
HON(^{3}A″)	−130.621 267	5.989	0.872	5.478
ClNO	−590.447 220	2.884	1.078	5.175
TS	−590.392 233	2.619	0.043	3.773
ClON	−590.409 170	2.740	0.385	4.140

[a] Total energy is in au, and all the hardness values are in eV.

Fock methods.[71−74] As shown in Figure 1, the NO bond length increases in going from HNO to TS and then shortens from TS to HON. The same bond length in the singlet state of minima and transition state is even shorter than that of the triplet state counterparts. In the case of ClNO, the NO bond is a minimum in the transition state structure and is larger in the ClNO form.

Concerning the energetical parameters, from the total B3LYP energy values (E) reported in Table 1, the barrier heights are calculated to be 75.38, 40.14, and 33.37 kcal/mol for HNO(^{1}A′), HNO(^{3}A″), and ClNO, respectively, while the isomerization energies are 40.66, 10.34, and 25.52 kcal/mol, respectively. The same quantities at the PWP86 level of theory are 70.54, 43.37, and 34.50 kcal/mol and 41.16, 12.55, and 23.88 kcal/mol (see Table 2). These values are in quantitative agreement with previous theoretical results.[75]

In Tables 1 and 2 are also reported the hardness, calculated by using different methods, and polarizability values of minima and transition states. The inspection of this table reveals that the trend predicted for critical points on the basis of MHP holds only for the ClNO system, for which the μ values at the extrema are close to one another. For the HNO system, in both ^{1}A′ and ^{3}A″ states, whatever the work definition is used for the computation of η, the relative stability of the isomers and transition state is not correctly reproduced. Moreover, the values obtained from the HOMO−LUMO energy difference at PWP86 level are close to zero. Polarizability values, on the other hand, do not follow any particular trend at the extrema.

It is also worth to note that the ^{3}A″ state for HNO is lower in energy than the ^{1}A′ state, while the order is reversed in the case of HON. Since the transition state for the ^{3}A″ isomerization is found to be lower than the ^{1}A′ one, the two surfaces must cross to an angle HNO greater than 54.2°. This two-state reaction behavior will be taken into account to explain the relationship between energy and reactivity indices profiles. To check the hardness and the polarizability behavior along the whole reaction path, the profiles of η and α for the above-mentioned reactions have been constructed. Also, the variation of the chemical potential and of the electronic (E_{el}) and nuclear (V_{nn}) components of the total energy has been considered. At the B3LYP level, the IRC tool has been used to draw the behavior of reactivity descriptors, while at the PWP86 level the reaction path for the isomerization of HNO and ClNO has been conveniently described by the variation of the HNO and ClNO angle (θ). From a comparison among the energy profiles reported in Figure

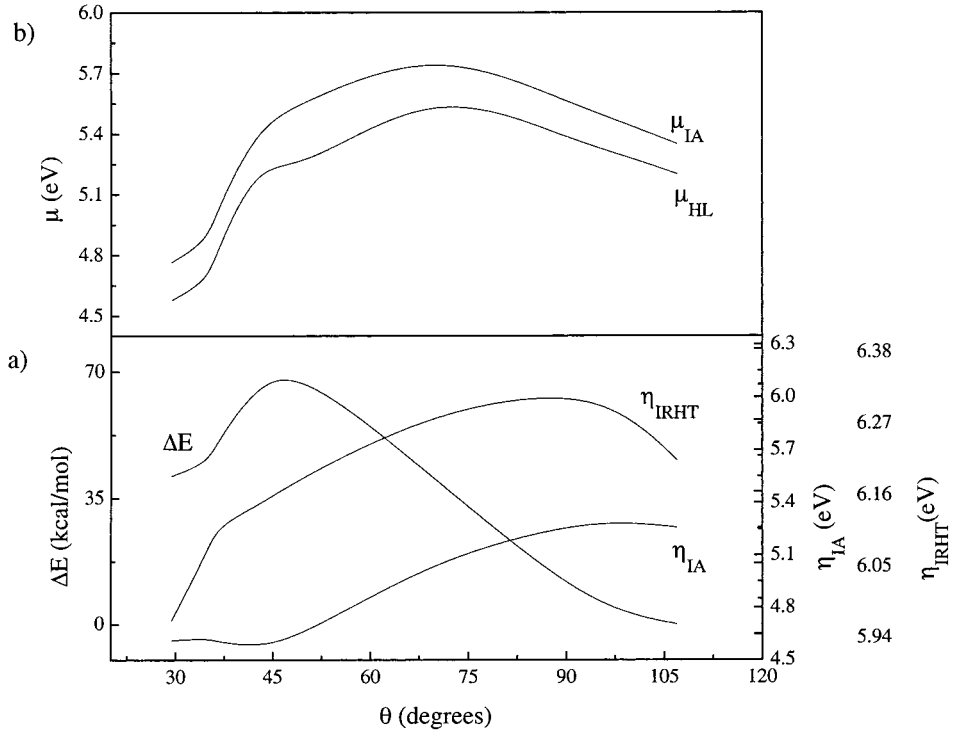

Figure 2. Plots of PWP86 (a) relative energies (left scale) and hardness (right scale) and (b) chemical potential against HNO (θ) angle for the HNO(^{1}A′) system.

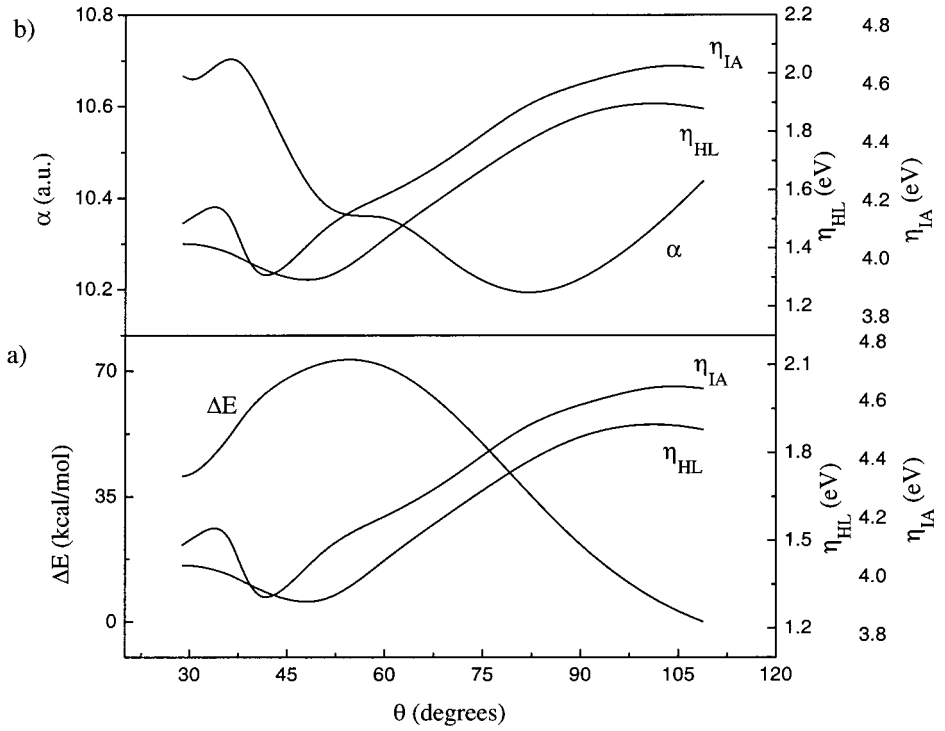

Figure 3. Plots of B3LYP (a) relative energies (left scale) and hardness (right scale) and (b) polarizability (left scale) and hardness (right scale) against HNO (θ) angle of the HNO(^{1}A′) system.

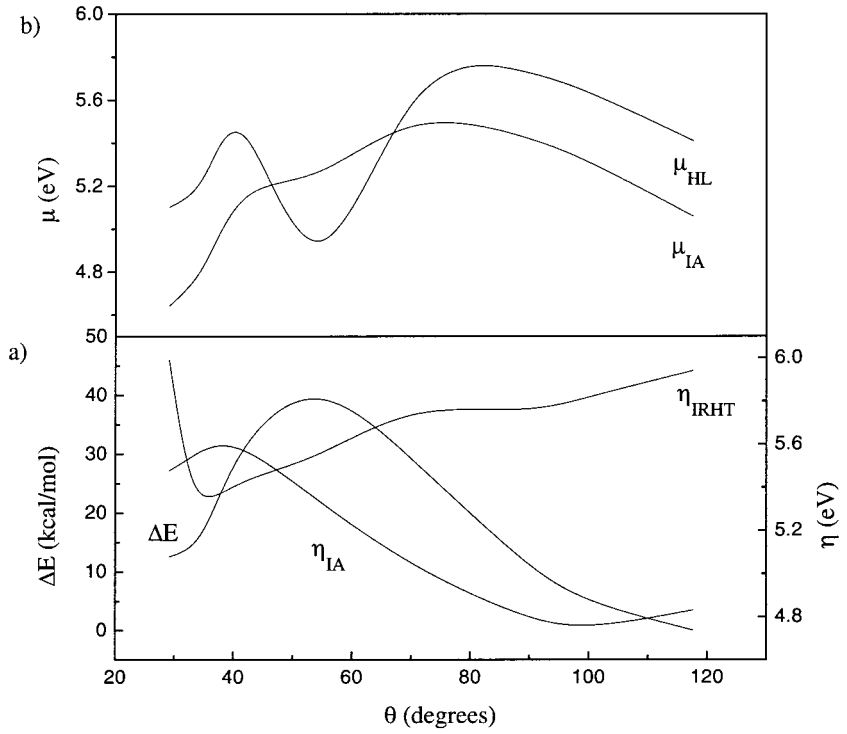

Figure 4. Plots of PWP86 (a) relative energies (left scale) and hardness (right scale) and (b) chemical potential against HNO (θ) angle for the HNO(^{3}A″) system.

2a and 3a, 4a and 5a, and 8a and 9a, it can be concluded that this approximation can be used for such relatively simple situations.

The nature of the PWP86 μ profiles, reported in Figures 2b, 4b, and 8b, calculated using both HL and IP−EA approximations, reveals that this quantity changes significantly along the reaction path during the isomerization reaction of HNO, in both its ^{1}A′ and ^{3}A″ states, and remains quite constant in the case of ClNO.

We first discuss the nature of the η and α profiles of the ^{1}A′ surface of HNO drawn in Figures 2a and 3a. The PWP86 HOMO−LUMO hardness profile is not reported because, as previously pointed out, the values are very close to zero. Except the behavior of η_{IRHT}, which is almost flat, all the other are characterized by the presence of two maxima and one minimum. They refer to HON and HNO minima and the transition state between them and occur at or near the corresponding points along the energy profiles. In all cases the minimum is shifted

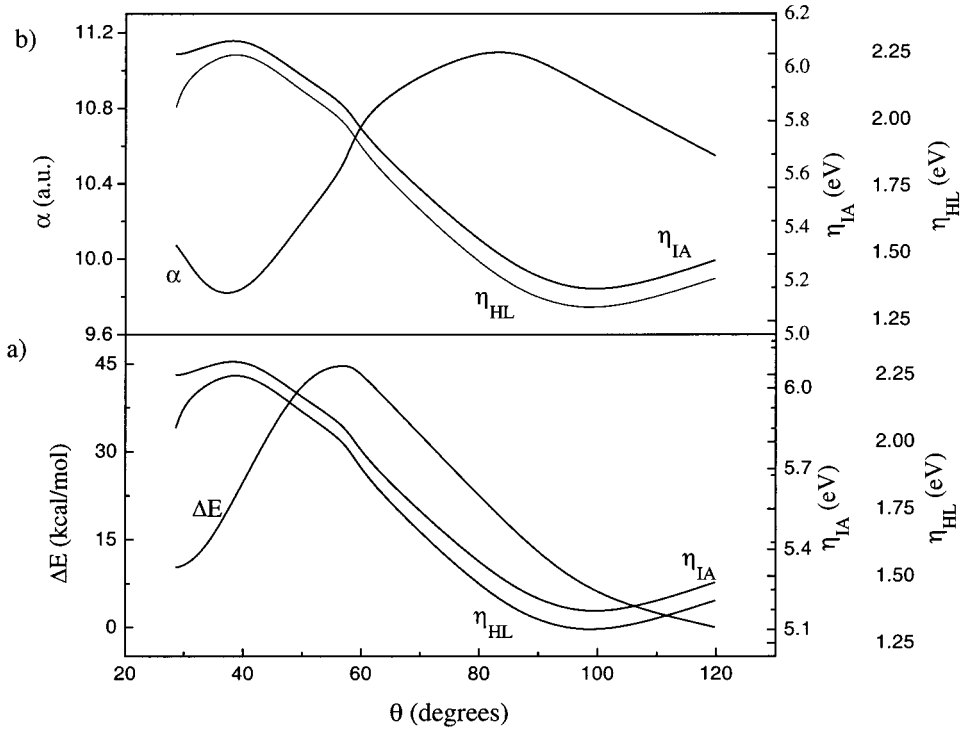

Figure 5. Plots of B3LYP (a) relative energies (left scale) and hardness (right scale) and (b) polarizability (left scale) and hardness (right scale) against HNO (θ) angle for the HNO(^{3}A″).

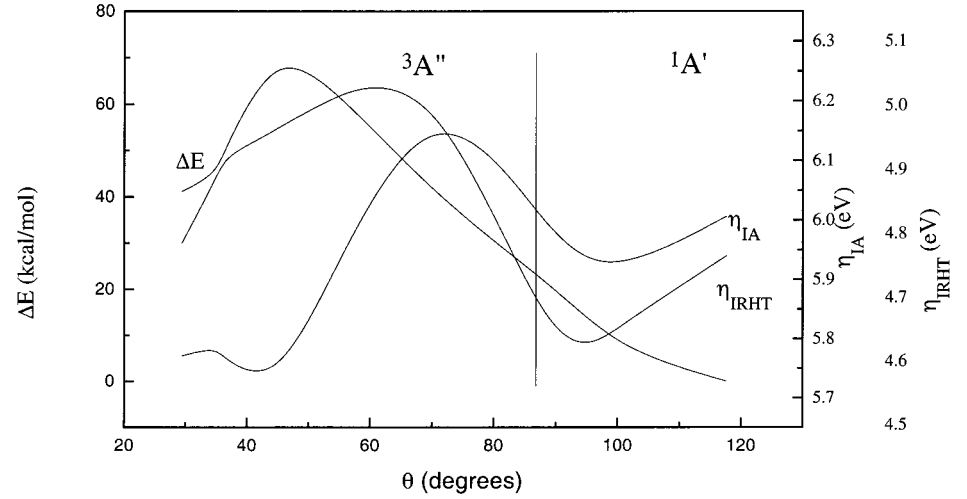

Figure 6. Plots of PWP86 (a) relative energies (left scale) and hardness (right scale) against HNO (θ) angle for the minimum energy path of the ^{1}A′ and ^{3}A″ states of HNO. These curves were simply obtained by linking the ^{3}A″ profiles of Figure 4, for θ values ranging between 30° and 86°, and the ^{1}A′ profiles of Figure 2, for θ values ranging between 86° and 120°.

toward the HON isomer with respect to the energy maximum. The B3LYP polarizability profile, sketched in Figure 3b, goes through a minimum and a maximum that do not coincide with the minimum and maximum of the potential energy surface. Also in this case the maximum in the α profile appears closer to the HON side compared to the position of the transition state. Comparison between η and α profiles shows that their changes do not follow the opposite trend, and it seems that the higher hardness−lower polarizability criterion does not hold in this situation.

To check the Parr and Gazquez statement,[52] the PWP86 electronic and nuclear energies as a function of the reaction coordinate, not shown, have been investigated. The extrema have been found to be coincident in most cases: V_{nn} is a maximum at the point where E_{el} is a minimum and vice versa. Indeed, they are nearly perfect mirrors of one another. Moreover, there is also a coincidence between the position of extrema in E_{el} and V_{nn} profiles and those in η_{IA} profiles.

Now, we focus our attention on the ^{3}A″ surface of the HNO isomerization reaction. Notwithstanding that all the hardness profiles, both at the B3LYP and PWP86 level, attain a minimum value, these extrema correspond to bond angles that do not match maxima of the potential energy surfaces (see Figures 4 and 5). Moreover, the stability order of the two minima is reversed in all cases. Polarizability shows minimum and maximum values that do not coincide with extrema in the energy profile. Neverthless, from Figure 5b it is clear that hardness and polarizability behaviors are opposite to each other along the reaction coordinate.

Also, in this case a possible relationship between the hardness and the electronic and nuclear energy profiles has been checked. At the PWP86 level the electronic energy has extrema at the

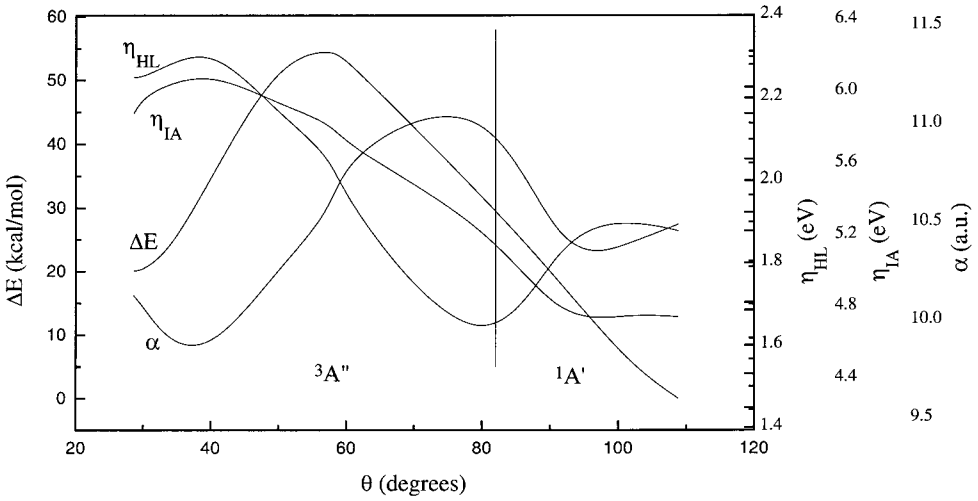

Figure 7. Plots of B3LYP relative energies (left scale) and hardness and polarizability (right scale) against HNO (θ) angle for the minimum energy path of the ^{1}A′ and ^{3}A″ states of HNO. These curves were simply obtained by linking the ^{3}A″ profiles of Figure 5, for θ values ranging between 30° and 82°, and the ^{1}A′ profiles of Figure 3, for θ values ranging between 82° and 110°.

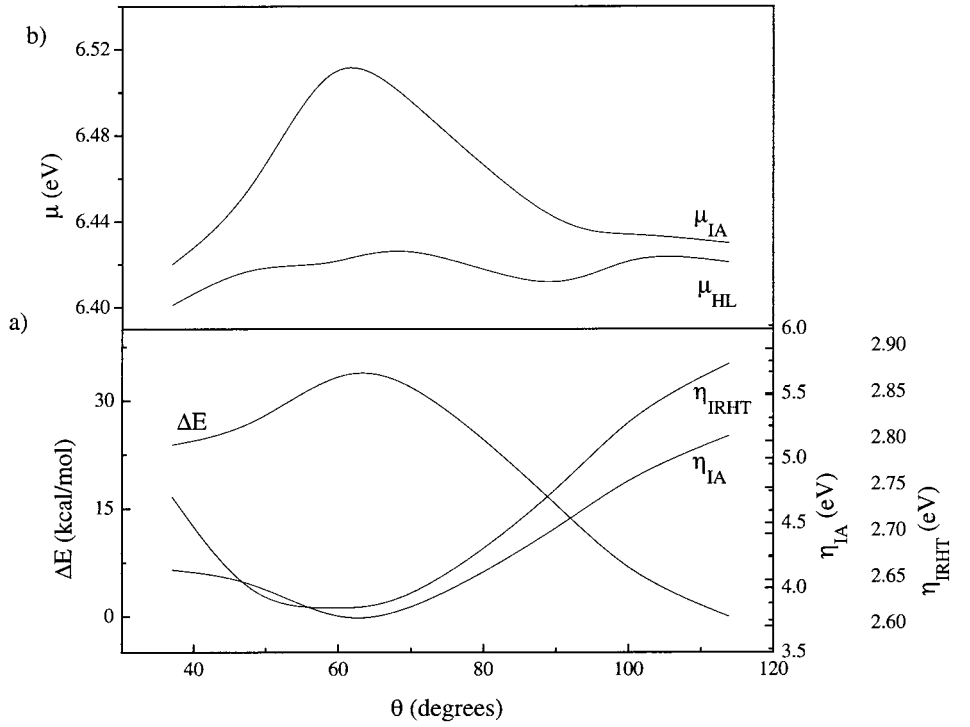

Figure 8. Plots of PWP86 (a) relative energies (left scale) and hardness (right scale) and (b) chemical potential against ClNO (θ) angle for the ClNO system.

same points that nuclear energy does, but the electronic energy goes through a maximum, a minimum for nuclear energy, at $\theta = 43.2°$ that does not correspond to a maximum of the η profiles.

The MHP is strictly applicable to the change in a system when it evolves from the ground state of one form to the ground state of another form. Due to the curve crossing between the ^{1}A′ and ^{3}A″ states, neither the former nor the latter potential energy curve represents the ground state over the whole reaction path. With the aim to examine the influence of crossing on the hardness and polarizability profiles, the minimum energy profiles for the two ^{1}A′ and ^{3}A″ states, in Figure 6 at the PWP86 level and in Figure 7 at B3LYP level, have been reported. In the same figures the corresponding hardness and polarizability variations have been plotted. These curves have a physical meaning since the reaction starts with the HON isomer in its triplet state and ends with HNO in its singlet state. None of the hardness profiles, whatever the method used for their computation, has a behavior closer to that required by MHP. The polarizability variation also does not obey the minimum polarizability principle. Nevertheless, it noteworthy that between the changes of η_{HL} and polarizability an inverse relationship exists through the IRC path.

The energetic and hardness profiles for the chlorine shift in ClNO are drawn in Figures 8a and 9a, as a function of the bond angle ClNO. All the η profiles are characterized by two maxima and a minimum. They refer to ClON, ClNO, and the transition state structure, respectively, and occur almost at the corresponding points in the energy profile. In this case also the behavior of the η_{IRHT} profile follows the correct trend, but again the

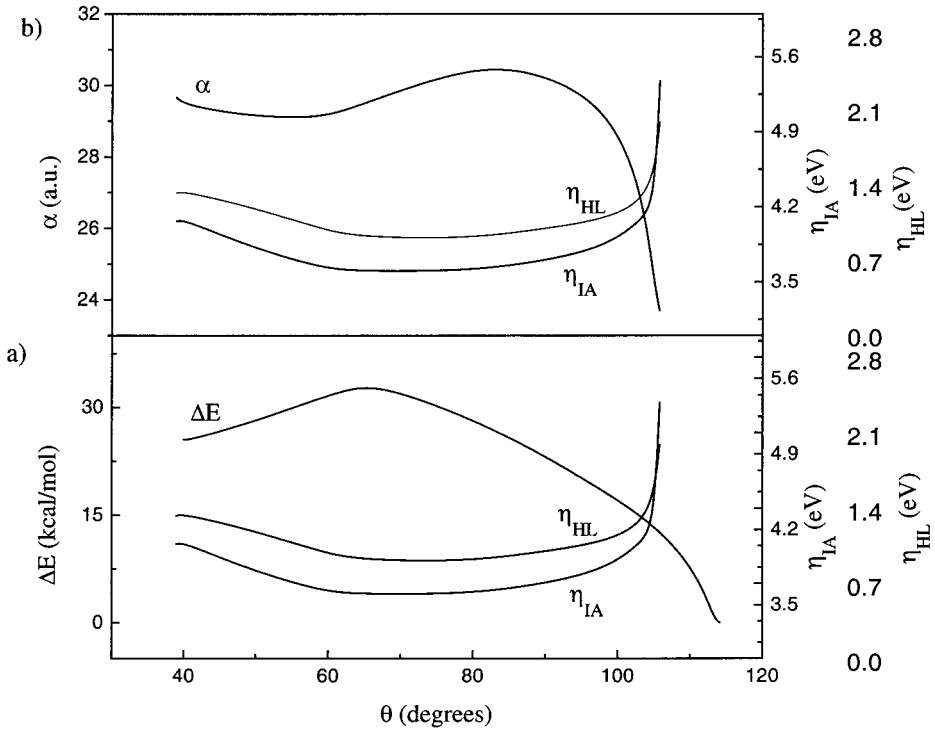

Figure 9. Plots of B3LYP (a) relative energies (left scale) and hardness (right scale) and (b) polarizability (left scale) and hardness (right scale) against ClNO (θ) angle for the ClNO system.

minimum is shifted toward the ClNO isomer compared with the maximum in energy. The constancy of the chemical potential (Figure 8b) can be considered responsible for the nicely opposite energy and hardness behavior. On the contrary, the polarizability profile does not match that of the energy, and an inverse relationship between polarizability and hardness is not evidenced in Figure 9b. In this case the behavior of E_{el} once again mirrors that of V_{nn} and the extrema in η_{IA} coincide with those in the two components of the total energy.

Conclusion

Two different chemical situations, namely a two-state reaction (HNO) and an isomerization reaction involving a system with ionic character (ClNO), have been studied with the aim to test the validity of MHP. The isomerization processes have been characterized through a study of the profiles of the energy, polarizability, chemical potential, and hardness. For the calculation of the latter quantities, different working formulas have been employed. On the basis of our results, it appears that MHP and MPP are not generally verified. The best situation is found in the case of the ClNO isomerization reaction, when the condition of constant chemical potential is fulfilled, because the energetic path has an opposite behavior than that of the hardness whatever method used for its computation. However, this conclusion cannot be extended to polarizability that does not follow a behavior in agreement with MPP. No general conclusion can be drawn about the existence of an inverse relation between hardness and polarizability. Much work is required to understand and assess the behavior of hardness and polarizability and, then, to predict changes of these properties for molecules along the reaction path.

Acknowledgment. This work was funded by MURST (Progetto Nazionale Sistemi a Grandi Interfasi) and by Università della Calabria.

References and Notes

(1) Parr, R. G.; Yang, W. *Density Functional Theory of Atoms and Molecules*; Oxford University Press: New York, 1989.
(2) Parr, R. G.; Donnelly, R. A.; Levy, M.; Palke, W. E. *J. Chem. Phys.* **1978**, *69*, 4491.
(3) Parr, R. G.; Pearson, R. G. *J. Am. Chem. Soc.* **1983**, *105*, 7512.
(4) Pearson, R. G. *J. Chem. Educ.* **1987**, *64*, 561.
(5) Pearson, R. G. *Acc. Chem. Rec.* **1993**, *26*, 250.
(6) Yang, W.; Lee, C.; Ghosh, S. K. *J. Phys. Chem.* **1985**, *89*, 5413.
(7) Balewander, R.; Komorowski, L. *J. Chem. Phys.* **1998**, *109*, 5203 and references therein.
(8) Nalewajski, R. F.; Korchowiec, J. *Charge Sensitivity Approach to Electronic Structure and Chemical Reactivity*; World-Scientific: Singapore, 1997 and references therein.
(9) Roy, R. K.; Pal, S.; Hirao, K. *J. Chem. Phys.* **1999**, *110*, 8236; **2000**, *113*, 1372.
(10) Chermette, H. *Coord. Chem. Rev.* **1998**, *178*−*180*, 699.
(11) Janak, J. F. *Phys. Rev.* B **1978**, *18*, 7165.
(12) Neshev, N.; Mineva, T. In *Metal*−*Ligand Interactions: Structure and Reactivity*; Russo, N., Salahub, D. R., Eds.; Kluwer: Dordrecht, 1996; p 361.
(13) Grigorov, M.; Weber, J.; Chermette, H.; Tronchet, J. M. J. *Int. J. Quantum Chem.* **1997**, *61*, 551.
(14) Galvan, M.; Dal Pino, A., Jr.; Joannopoulos, J. D. *Phys. Rev. Lett.* **1993**, *70*, 21.
(15) Mineva, T.; Russo, N.; Sicilia, E.; Toscano, M.; *J. Chem. Soc., Faraday Trans.* **1997**, *18*, 3309.
(16) Mineva, T.; Russo, N.; Sicilia, E.; Toscano, M. *Theor. Chem. Acc.* **1999**, *101*, 388.
(17) Russo, N.; Toscano, M.; Grand, A.; Mineva, T. *J. Phys. Chem. A* **2000**, *104*, 4017.
(18) Marino, T.; Russo, N.; Sicilia, E.; Toscano, M.; Mineva, T. *Adv. Quantum Chem.* **2000**, *36*, 93.
(19) Grigorov, M. G.; Weber, J.; Vulliermet, N.; Chermette, H.; Tronchet, J. M. J *J. Chem. Phys.* **1998**, *108*, 8790.
(20) Chermette, H. *J. Comput. Chem.* **1999**, *20*, 129.
(21) Pearson, R. G. *Chemical Hardness: Applications from Molecules to Solids*; Wiley-VCH Verlag GMBH: Weinheim, 1997; and references therein.
(22) De Proft, F.; Langeneaker, W.; Geerlings, P. *J. Phys. Chem.* **1993**, *97*, 1826.
(23) Chattaraj, P. K.; Nath, S.; Sannigrahi, A. B. *Chem. Phys. Lett.* **1993**, *212*, 223.
(24) Parr, R. G.; Chattaraj, P. K. *J. Am. Chem. Soc.* **1991**, *113*, 1855.

(25) Chattaraj, P. K.; Liu, G. H.; Parr, R. G. *J. Phys. Chem*. **1995**, *237*, 171.
(26) Sebastian, L. *Chem. Phys. Lett.* **1994**, *231*, 40.
(27) Parr, R. G.; Yang, W. *Annu. Rev. Phys. Chem.* **1995**, *46*, 701.
(28) Liu, G. H.; Parr, R. G. *J. Chem. Phys*. **1997**, *106*, 5578.
(29) Datta, D. *J. Phys. Chem.* **1992**, *96*, 2409.
(30) Pal, N.; Vaval, N.; Roy, S. *J. Phys. Chem.* **1993**, *97*, 4404.
(31) Chattaraj, P. K.; Nath, S.; Sannigrahi, A. B. *J. Phys. Chem.* **1994**, *98*, 9143.
(32) Cardenas-Jiròn, G. I.; Toro-Labbè, A. *J. Phys. Chem.* **1995**, *99*, 12730.
(33) Kar, T.; Scheiner, S. *J. Phys. Chem.* **1995**, *99*, 8121.
(34) Ghanty, T. K.; Ghosh, S. K. *J. Phys. Chem*. **1996**, *100*, 12295.
(35) Cardenas-Jiròn, G. I.; Gutierrez-Oliva, S.; Melin, J.; Toro-Labbè, A. *J. Phys. Chem.* **1997**, *101*, 4621.
(36) Kar, T.; Scheiner, S.; Sannigrahi, A. B. *J. Phys. Chem.* **1998**, *102*, 5967.
(37) Chandra, A. K.; Nguyen, M. T. *J. Phys. Chem.* **1998**, *102*, 6181.
(38) Mineva, T.; Russo, N.; Sicilia, E. *J. Am. Chem. Soc*. **1998**, *120*, 9053.
(39) Cardenas-Jiròn, G. I.; Gutierrez-Oliva, S.; Letelier, J. R.; Toro-Labbè, A. *Mol. Phys.* **1999**, *96*, 61.
(40) Mineva, T.; Neshev, N.; Russo, N.; Sicilia, E.; Toscano M. *Adv. Quantum Chem.* **1999**, *33*, 273.
(41) Le, T. N.; Nguyen, L. T.; Chandra, A. K.; De Proft, F.; Geerlings, P.; Nguyen, M. T. *J. Chem. Soc., Perkin Trans. 2* **1999**, 1249.
(42) Nguyen, L. T.; Le, T. N.; De Proft, F.; Chandra, A. K.; Langeneaker, W.; Nguyen, M. T.; Geerlings, P. *J. Am. Chem. Soc.* **1999**, *121*, 5992.
(43) Chattaraj, P. K.; Fuentelba, P.; Gomez, B.; Contreras, R. *J. Am. Chem. Soc.* **2000**, *122*, 348.
(44) Toro-Labbè, A. *J. Phys. Chem.* **1999**, *103*, 4398.
(45) Ghanty, T. K.; Ghosh, S. K. *J. Phys. Chem.* **2000**, *104*, 2975.
(46) Politzer, P. *J. Chem. Phys.* **1987**, *86*, 1072.
(47) Hati, S.; Datta, D. *J. Phys. Chem.* **1994**, *98*, 10451; **1995**, *99*, 10742.
(48) Kohn, W.; Sham, L. *J. Phys. Rev.* **1965**, *140*, A1133.
(49) Chattaraj, P. K.; Fuentelba, P.; Jaque, P.; Toro-Labbè, A. *J. Phys. Chem.* **1999**, *103*, 9307.
(50) Champagne, B.; Perpete, E. A.; Jacquemin, D.; van Gisbergen, S. J. A.; Baerends, E. J.; Soubra-Ghaoui, C.; Robins, K. A.; Kirtman, B. *J. Phys. Chem A* **2000**, *104*, 4755.
(51) Vedernikova, I.; Proynov, E.; Salahub, D.; Haemers, A. *Int. J. Quantum Chem*., **2000**, *77*, 161.
(52) Parr, R. G.; Gazquez, J. L. *J. Phys. Chem.* **1993**, *97*, 3939.
(53) Gazquez, J. L. *Struct. Bond.* **1993**, *80*, 27.
(54) Kohn, W.; Becke, A. D.; Parr, R. G. *J. Phys. Chem.* **1996**, *100*, 12974.
(55) Baerends, E. J. *Theor. Chem. Acc*. **2000**, *103*, 265.
(56) Stowasser, R.; Hoffmann, R. *J. Am. Chem. Soc.* **1999**, *121*, 3414.
(57) Slater, J. C. *The Self-Consistent Field for Molecules and Solids*; McGraw-Hill: New York, 1974; Vol.4.
(58) Liu, G. H.; Parr, R. G. *J. Am. Chem. Soc*. **1995**, *117*, 317
(59) Cohen, H. D.; Roothan, C. C. J. *J. Chem. Phys.* **1965**, *43*, S34.
(60) Becke, A. D. *J. Chem. Phys.* **1993**, *98*, 5648.
(61) Lee, C.; Yang, W.; Parr, R. G.*Phys. Rev. B* **1988**, *37*, 785.
(62) Frish, M. J.; Trucks, G. W.; Schlegel, H. B.; Gill, P. M. W.; Johnson, B. G.; Robb, M. A., Cheesman, J. R.; Keith, T. A.; Petersson, G. A.; Montgomery, J. A.; Raghavachari, K.; Al-Laham, M. A.; Zakrzewski, V. G.; Ortiz, J. V.; Foresman, J. B.; Croslowski, J.; Stefanov, B. B.; Nanayakkara, A.; Challacombe, M.; Peng, C. Y.; Ayala, P. Y.; Chen, W.; Wong, M. W.; Andres, J. L:, Peplogle, E. S.; Gomperts, R.; Martin, R. L.; Fox, D. J.; Binkley, J. S.; Defrees, D. J.; Baker, J.; Stewart, J. P.; Head-Gordon, M.; Gonzales, C.; Pople, J. A. *Gaussian 94* (Revision A.1) Gaussian, Inc.: Pittsburgh, PA, 1995.
(63) Perdew, J. P.; Wang, Y. *Phys. Rev*. **1986**, *B33*, 8800.
(64) Perdew, J. P. *Phys. Rev.* **1986**, *B33*, 8822.
(65) Godbout, N.; Salahub, D. R.; Andzelm, J.; Wimmer, E. *Can. J. Chem*. **1992**, *70*, 560.
(66) St-Amant, A. *Ph.D. Thesis*; Universite de Montreal: Canada, **1992**.
(67) Broyden, C. C. *J. Inst. Math. Appl*. **1970**, *6*, 76; Fletcher, R. *Comput. J.* **1970**, *13*, 317; Goldfarb, D. *Math. Comput.* **1970**, *24*, 1385.
(68) Abashkin, Y.; Russo, N. *J. Chem. Phys.* **1994**, *100*, 4477.
(69) Dalby, W. *J. Chem. Phys.* **1958**, *36*, 1336.
(70) Sengputa, D.; Chandra, A. K. *J. Chem. Phys.* **1994**, *101*, 3906 and references therein.
(71) Guadagnini, R.; Schatz, G. C.; Walch, S. P. *J. Chem. Phys.* **1995**, *102*, 774 and references therein.
(72) Lee, T. J. *J. Chem. Phys.* **1993**, *99*, 9783.
(73) Meredith, C.; Davy, R. D.; Schaefer, H. F., III *J. Chem. Phys.* **1990**, *93*, 1215.
(74) Alikhani, M. E.; Dateo, C. E.; Lee, T. J. *Chem. Phys. Lett.* **1998**, *292*, 35.
(75) Meredith, C.; Quelch, G. E.; Schaefer, H. F., III *J. Chem. Phys.* **1992**, *96*, 480.